Nonadiabatic Excited State Molecular Dynamics with explicit solvent: NEXMD-SANDER implementation

Dustin A. Tracy[1], Sebastian Fernandez Alberti[2], Johan Fabian Galindo[3], Sergei Tretiak[4] and Adrian E. Roitberg[1,5*]

[1]Department of Chemistry, University of Florida, Gainesville, Florida 32611, United States
[2]Universidad Nacional de Quilmes/CONICET, Roque Saenz Peña 352, B1876BXD Bernal, Argentina
[3]Departamento de Química, Universidad Nacional de Colombia, Sede Bogotá, 111321 Bogotá, Colombia.
[4]Theoretical Division, Center for Nonlinear Studies (CNLS) and Center for integrated Nanotechnologies (CINT), Los Alamos National Laboratory, Los Alamos, New Mexico 87545, United States
[5]CONICET─Universidad de Buenos Aires, Instituto de Química-Física de los Materiales, Medio Ambiente y Energía (INQUIMAE), Ciudad Universitaria, Pabellón 2, Buenos Aires C1428EHA, Argentina

*corresponding author: roitberg@ufl.edu

ABSTRACT

In this article, the Nonadiabatic Excited-state Molecular dynamics (NEXMD) package is linked with the SANDER package, provided by AMBERTOOLS. The combination of these software packages enables the simulation of photoinduced dynamics of large multichromophoric conjugated molecules involving several coupled electronic excited states embedded in an explicit solvent by using Quantum/Mechanics/Molecular Mechanics (QM/MM) methodology. The fewest switches surface hopping algorithm, as implemented in NEXMD, is used to account for quantum transitions among the adiabatic excited-states Simulations of the photoexcitation and subsequent nonadiabatic electronic transitions and vibrational energy relaxation of a substituted polyphenylene vinylene oligomer (PPV3-NO2) in vacuum and methanol as explicit solvent has been used as a test case. The impact of including specific solvent molecules in the QM region is also analysed. Our NEXMD-SANDER QM/MM implementation provides a useful computational tool to simulate qualitatively solvent-dependent effects, like electron transfer, stabilization of charge separated excited states, the role of solvent reorganization in the molecular optical properties, observed in solution-based spectroscopic experiments.

INTRODUCTION

Understanding the photoinduced mechanisms of nonadiabatic electronic and vibrational relaxation and energy redistribution in organic chromophoric molecules has a significant impact on the development of new synthetic materials with potential technological implications like organic light-emitting diodes (LEDs) and solar cells [1,2,3], photoconversion[4,5], imaging[6] and sensing[7], among others. These functionalities can be conditioned by the effect of explicit solvent environments that modify the absorption and emission properties of solutes by their interaction with specific solvent molecules[8]. The environment can significantly modify photophysical dynamics aspects[9] associated to their ultrafast intra- and/or inter-molecular energy transfer fluxes.[10,11,12]. The efficiency of ultrafast nonradiative relaxation channels depends on the amount of energy dissipation among the solvent/bath degrees of freedom, solvent-driven coherent population transfers[13], transient stabilizations of specific charge separated excited states[14], relative time-scales of solvent reorientation[15] and molecular energy/charge transfer.

The nonadiabatic dynamics of organic chromophoric molecules in solution is affected by the solvent. The electronic states of the solvent can couple to the states of the solute, introducing changes in the excited-state electronic densities, in the potential energy surfaces topographies, energy dissipation and trigger new energy/charge transfer flows[16,17]. Thus, the solvent molecules around the chromophore may qualitatively modify the nonadiabatic relaxation compared to an isolated excited molecule. Solvent-driven charge delocalization and confinement may create different relaxation pathways to the lower-energy electronic states, excited-state mixing and population splitting of nuclear wavepackets that can ultimately lead to significant changes in its fluorescent properties[18,19].

Implicit solvent approximations, such as polarizable continuum models,[20, 21] can partially resolved this issue by effectively incorporating solute-solvent interactions into electronic structure calculations.[22, 23] These methods, while promising, cannot accurately account for the rotational relaxation and motion of local solvent molecules, steric interactions, non-equilibrium and state-specific solvation[24,25]. An attractive alternative is the use of hybrid Quantum Mechanics/Molecular Mechanics (QM/MM) methods[19,26,27,28,29,30,31,32,33] that limit QM calculations to a certain area of interest while the rest of the system is treated classically using MM. Importantly, common on-the-fly QM/MM molecular dynamics schemes routinely incorporate interactions between QM and MM regions. Despite decades of development, modeling dynamical processes beyond Born-Oppenheimer approximation remains computationally challenging task for QM/MM frameworks. While different theoretical options can tackle nonadiabatic processes in condensed phase[34,35,36] a combination of QM/MM methods with surface hopping algorithm is likely the most extensively applied[37,17,38,39,19,40,41,42]. Mixed quantum-classical surface hopping methodologies, by drastically reducing the computational costs with respect to full quantum-mechanical or semiclassical approaches, allows atomistic simulations of larger systems and longer time scales[43,10,44,45]. Moreover, since it does not require pre-calculated

potential energy surfaces, it is ideal for implementing *on-the-fly* nonadiabatic dynamics schemes[46,47,48,49,50,51,52,53].

Non-adiabatic EXcited-state Molecular Dynamics (NEXMD)[54,10] is an efficient computational code that has been developed for simulating photoinduced dynamics and non-radiative relaxation of large chromophoric conjugated molecular systems involving manifolds of coupled electronic excited states over timescales up to tens of picoseconds. NEXMD incorporates several algorithms that extend modeling beyond the Born-Oppenheimer approximation. It allows the treatment of solvent effects using implicit models[20,21] and, more recently, the NEXMD-SANDER implementation[55] allows to use QM/MM methods during *adiabatic* excited state molecular dynamics simulations with tens of thousands of MM atoms by linking NEXMD to the SANDER package supplied by the AMBERTOOLS of the AMBER molecular dynamics package.[56]

Herein, we extend the NEXMD-SANDER QM/MM framework to enable calculations of *nonadiabatic* dynamics using surface hopping approach as it is implemented in NEXMD[52]. The use of semiempirical model Hamiltonians and Configuration Interaction Singlets (CIS) or Random Phase Approximation (RPA), that adequately account for essential correlation effect in excited electronic states, allows us to consider ~200 atoms in the QM region, and 1000s of atoms at the MM partition. As in our previous studies[21,20,55] and for the sake of comparison, the acceptor substituted polyphenylene vinylene oligomer (PPV3-NO_2) (shown in **Figure 1**) is used as a test case. A major feature of PPV oligomers is the sensitivity of their nonadiabatic characteristics like charge transfer character and donor-acceptor groups present to the environment[57] making them prototype tunable materials in optoelectronic devices.[58,59,60,61,62]

SANDER-NEXMD QM/MM FOR NONADIABATIC DYNAMICS

NEXMD overview

NEXMD (Nonadiabatic EXcited-state Molecular Dynamics) is a computational package developed to simulate excited-state dynamics beyond Born-Oppenheimer approximation. It combines non-adiabatic drivers such as trajectory surface hopping (TSH), Ehrenfest, and Ab Initio Multiple Cloning approaches[63] with "on the fly" analytical calculations of excited state energies, gradients and non-adiabatic coupling terms (NACT) at the configuration interaction singles (CIS) level with the semiempirical Hamiltonian models (AM1, PM3, MNDO).[10,54] In this contribution we focus on TSH technique[64,65]. As it is implemented in NEXMD, TSH adapts propagation of classical nuclei using Newtonian-like equation of motion. In contrast, the electronic wave function $\psi(t) = \sum_\alpha c_\alpha(t)\phi_\alpha$ is described quantum-mechanically using the basis of adiabatic CIS electronic states with wavefunctions ϕ_α, which evolves according to the time-dependent Schrödinger equation:

$$i\hbar\dot{c}_\alpha(t) = c_\alpha(t)E_\alpha - i\hbar\sum_\beta c_\beta(t)\boldsymbol{v}\cdot\boldsymbol{d}_{\alpha\beta} \qquad (1)$$

with E_α being the energy of the α^{th} CIS adiabatic electronic excited state. The non-adiabatic coupling terms are defined as $\left(\mathrm{NACT}_{\alpha\beta}\right) = \boldsymbol{v}\cdot\boldsymbol{d}_{\alpha\beta}$ with $\boldsymbol{v}$ being the nuclear

velocities and the non-adiabatic derivative coupling vectors $\left(\mathrm{NACR}_{\alpha\beta}\right)$ are defined as $\boldsymbol{d}_{\alpha\beta} = \langle\phi_\alpha|\nabla_{\boldsymbol{r}}\phi_\beta\rangle$.

NEXMD calculates transition density matrices throughout the molecular dynamics simulations. These quantities are defined in the atomic orbital (AO) basis[66] as $(\rho^{0\alpha})_{ij} = \langle\phi_\alpha|c_i^\dagger c_j|\phi_0\rangle$, with ϕ_0 and ϕ_α being the wavefunctions corresponding to the adiabatic ground- and CIS excited- states, respectively, $c_i^\dagger$ and c_j are the respective creation and annihilation operators acting over AOs i and j. More details about the NEXMD theory, implementation, advantages and testing parameters can be found in our previous works.[10,54,67]

QM/MM and nonadiabatic dynamics.

The QM/MM implementation in SANDER[68] divides the entire molecular system into QM and MM regions. In our new NEXMD-SANDER QM/MM implementation for nonadiabatic dynamics, the nuclei of the QM region are propagated classically on a single adiabatic QM-CIS electronic state, modified, at any given time, by the presence of the field created by the MM point charges. Hops from one adiabatic CIS state to another are governed by the coefficients of the electronic wave function, which is propagated quantum mechanically according to eq. (1), using the TSH approach as described above[67]. The QM energy and forces are computed using the electronic density of a particular electronic state, i.e. the *current state* according to the TSH prescription, of the QM part in the presence of MM charges. Nuclei of the MM region are propagated classically using AMBER's Molecular Mechanics (MM) force field.[56]

As in our previous work[55], the electronic Hamiltonian associated to short range interactions (defined according to a selected cutoff) between the QM charge density and MM atoms, treated as fixed point charges, is written as

$$\begin{aligned}\boldsymbol{H}_{QM/MM} = &-\sum_i\sum_m q_m\,\hat{\mathrm{h}}_{electron}(\bar{r}_i,\bar{r}_m)\\ &+\sum_k\sum_m q_k q_m\hat{\mathrm{h}}_{core}(\bar{r}_k,\bar{r}_m)\\ &+\sum_m\sum_k\left(\frac{A_{km}}{r_{km}^{12}}-\frac{B_{km}}{r_{km}^{6}}\right),\end{aligned} \qquad (2)$$

where index i corresponds to electrons, m to MM atoms with MM charge q_m, and k to the QM nuclei with charge q_k. A and B are the Lennard-Jones interaction parameters where r_{km} is the distance between the MM and QM atoms. $\hat{h}_{electron}$ represents the interactions between the MM charges and charge density of the QM region while $\hat{h}_{core}$ represents the electronic interactions between the MM charges and the core of the QM atoms.

For short-range interactions, the second term in eq. (2) is straightforwardly added to the Fock matrix elements of the *in-vacuo* QM region, $F_{\mu\nu}$, with μ and ν representing atomic orbitals, as

$$F_{\mu\nu}^{SR} = F_{\mu\nu} + \sum_m \frac{Z_m}{r_{\nu m}} \qquad (3)$$

with Z_m being the charge of the m^{th} nuclei of the MM region.

For the long range Coulombic interaction, the Particle Mesh Ewald method[69,70] considering Mulliken point charges for the QM region are used according to the SANDER SQM's (Semiempirical Quantum Mechanics) implementation when using periodic boundary conditions (PBC). These interactions are also added to the Fock matrix to get the complete QM/MM Fock matrix

$$F_{\mu\nu}^{QM/MM} = F_{\mu\nu}^{SR} + \frac{\partial}{\partial_{\mu\nu}}(\Delta E^{PBC}[Q,Q] + \Delta E^{PBC}[Q,q]) \qquad (4)$$

where $\Delta E^{PBC}[Q,Q]$ describes the corrections, due to the PBC applied to the QM atoms, treated as Mulliken charges (Q) and $\Delta E^{PBC}[Q,q]$ the corresponding corrections due to the MM atom's point charges. Since $\Delta E^{PBC}[Q,Q]$ depends on the Mulliken charges of the QM atoms, which are dependent on the trace of the density matrix of the current excited state, it can be calculated at each time step once the density matrix is obtained. The correction $\Delta E^{PBC}[Q,q]$ is simply the Coulombic potential from the periodic MM atoms. It is not dependent on the Mulliken charges of the QM atoms and as such can be added to the Fock matrix before the Self-Consistent Field (SCF) routine along with the short-range electrostatic correction.

SANDER-NEXMD interface design

Initial coordinates and velocities, and AMBER's parameters are introduced according to the standard SANDER MD input format with a new additional flag indicating that NEXMD is used for QM/MM simulations. The # N of electronic excited states, initial values for electronic coefficients $c_\alpha(0)$ (α=1,N) and other parameters related to the calculation of excited state electronic energies, gradients, coordinates and velocities of atoms of the QM region, NACTs, and propagation of electronic wavefunction are introduced in the NEXMD input file. SANDER sends the system coordinates and MM partial charges to NEXMD and then NEXMD calculates the QM electronic excited state energies, gradients and CIS transition density matrices ϕ_α (α=1,N). The SCF routine incorporates the effect of the MM molecules in the one electron terms of $\boldsymbol{H}_{QM/MM}$ atoms through the Fock matrix using eqs. (3) and (4) and it also computes the two-electron integrals. The modified ϕ_α are used to calculate the gradient of the QM atoms on the *current electronic state* and the NACTs. $\psi(t)$ is propagated using NEXMD with time step $\delta t = \Delta t/N_q$ respectively, where N_q is the number of quantum steps per classical step Δt. NEXMD evaluates the probabilities to hop according to the standard TSH prescription and, if a hop occurs, the QM nuclei will continue their propagation on the new state. Lennard-Jones interactions between MM and QM atoms are calculated by SANDER assigning the corresponding classical AMBER parameters to all atoms (both QM and MM). Finally, SANDER performs the coordinate and velocity propagation of all atoms and performs the total energy calculation. This cycle is repeated at each time step Δt throughout the nonadiabatic molecular dynamics simulation (see **Scheme 1**).

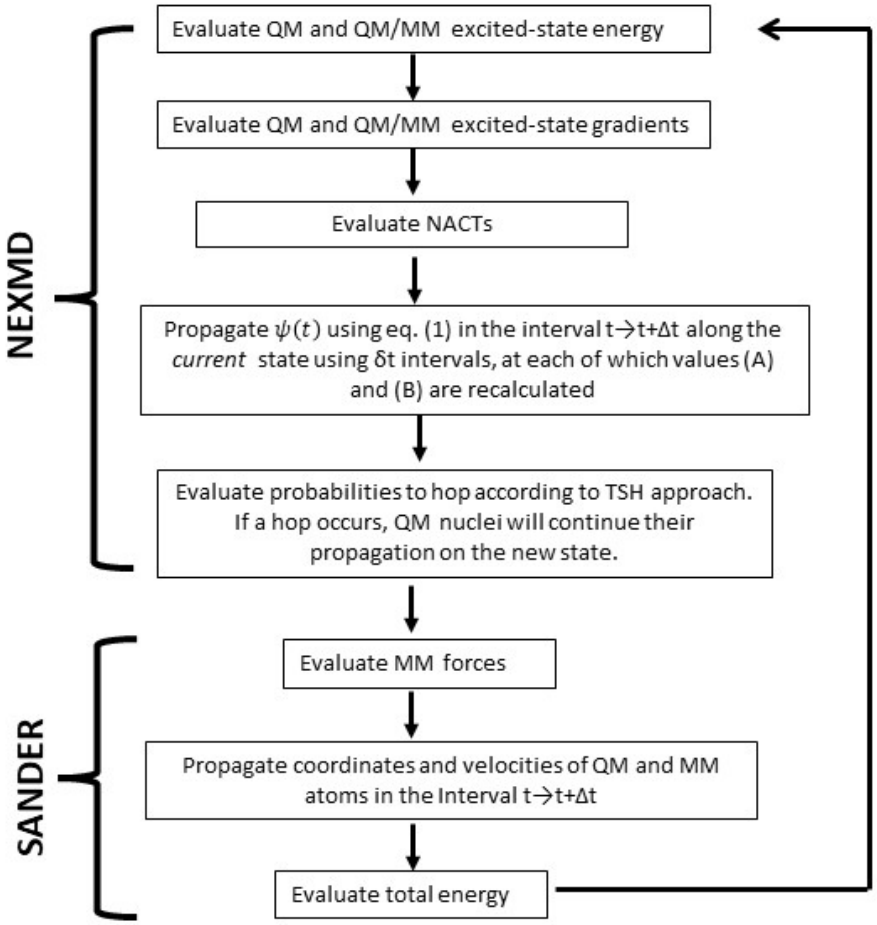

Scheme 1: Swimlane flowchart of SANDER-NEXMD QM/MM nonadiabatic simulations showing the cycle repeated at each interval Δt throughout the molecular dynamics.

NONADIABATIC EXCITED-STATE DYNAMICS OF PPV3-NO2

Computational details

Nonadiabatic excited state dynamics of PPV3-NO_2 (**Figure 1**, top panel) in explicit solvent has been simulated using the new NEXMD-SANDER QM/MM implementation with the semiempirical AM1 Hamiltonian model and CIS description of excited states.[71] This approach has been previously successfully applied to a large variety of chromophoric conjugated molecular systems[10,67] including a variety of different PPV oligomers[72,67] and PPV3-NO_2 using implicit solvent[20] as well as QM/MM adiabatic excited-state dynamics[55]. Following our previous article results[55], methanol has been chosen as solvent and up to10 solvent molecules were included in the QM region. Previous tests have shown minimal differences in the results between 10 and 20 solvent molecules in the QM region during excited state adiabatic dynamics.

Initial conditions were collected from 512 snapshots obtained every 2 ps from two 1024 ps of ground state dynamics trajectories equilibrated at 300K in vacuo and in methanol using the general AMBER force field for MM region, ground-state Hamiltonian for QM region and periodic boundary conditions. From each of these collected snapshots, 4 ps of QM in vacuo and QM/MM in methanol simulations using AM1 ground state Hamiltonian were performed.

The S_1 state is a primary band gap excitonic state in PPV oligomers[73]. The absorption from the S_1 state reveals a single absorbance feature separated from the S_1 band by 1.35 eV which is assigned as the so-called S_m band and frequently probed by transient absorption spectroscopies in similar systems. The main contribution to the absorbance from the S_1 state corresponds to S_9 and S_{10} states. **Figure 1** shows the contribution of these states calculated in vacuo and considering 0, 5 and 10 methanol molecules in the QM region. The solvent blueshifts the peak absorption spectra by around 0.1 eV indicating a desestabilization of high-energy excited states with respect to S_1 state. Importantly, this effect is introduced essentially by MM region: the number of solvent molecules included in the QM region has a negligible effect on this shift.

For each excited state trajectory, the initial excited state is then selected according to a Frank-Condon window given by $g_\alpha(\boldsymbol{r},\ \boldsymbol{R}) = f_\alpha \exp[-T^2(E_{laser} - E_\alpha)^2]$, where E_{laser} is the energy of a laser pulse from S_1 state centred at 1.35 eV (see **Figure 1**) and f_α is the oscillator strength of the α^{th} state. A Gaussian laser pulse, $f(t) = \exp(-t^2/2T^2)$, with $T = 424.63$ fs, corresponding to a FWHM (Full Width at Half Maximum) of 100 fs, was used. A classical time step of Δt = 0.5 fs for nuclei propagation with a Langevin thermostat with a friction constant of 2 ps^{-1} have been used for both ground-state and excited-state QM/MM simulations and a quantum time step of δt=0.1fs to propagate the electronic coefficients (eq. 1).[74] Decoherence[75] and trivial unavoided crossings[76] were treated as described elsewhere.[54]

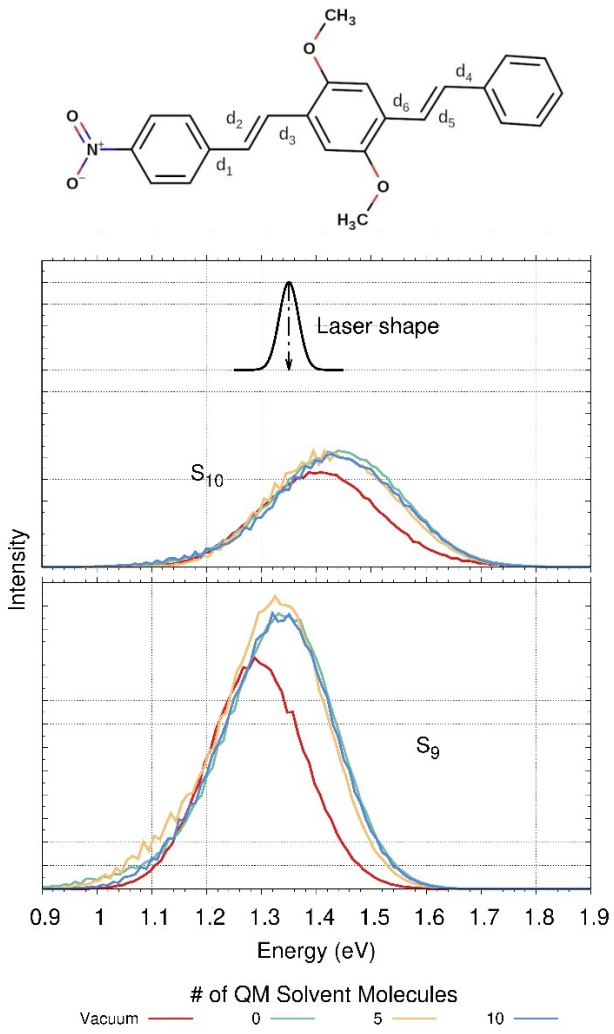

Figure 1. The calculated absorption of S_9 and S_{10} states from the first excited state S_1. The laser shape and wavelength is indicated in black.

Internal conversion.

Nonadiabatic excited state molecular dynamics simulations were performed for PPV3-NO_2 in vacuum and in methanol solvent after photoexcitation to the S_m band. **Figure 2** presents the evolution of the average electronic energy computed over all trajectories. It shows that the presence of MM region representing solvent molecules, dissipates the initial excitation energy slightly faster than vacuum, while the actual number of solvent molecules being treated as MM or QM makes no real difference.

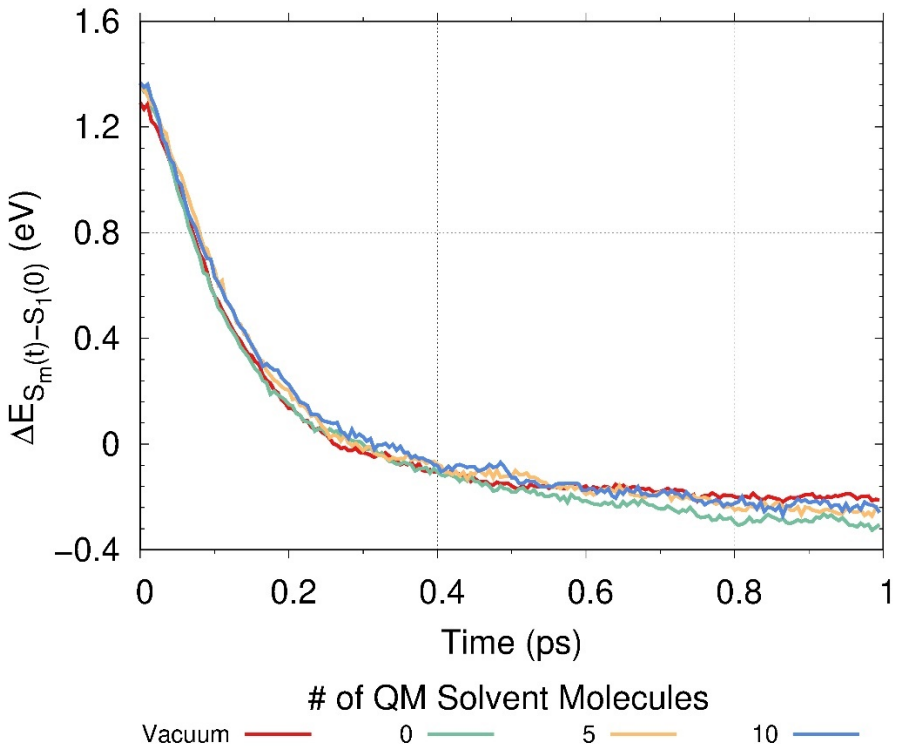

Figure 2. Evolution in time of the average electronic potential energy during the nonadiabatic excited state dynamics after photoexcitation to the S_m band.

Figure 3 shows the evolution in time of the average populations of different electronic states obtained from the fraction of trajectories in each state after the initial photoexcitation to the S_m band. Almost 85% of the initial excitation is localized on the S_9 state and the remaining fraction is on S_{10}. These initial populations experience ultrafast decays during the first ~250 fs that it is only slightly accelerated by the solvent and changes in the number of methanol molecules included in the QM region. The solvent effect is more pronounced on S_2. The latter represents the only intermediate state that transiently accumulates a significant amount of population. The presence of solvent molecules increases its transient population and slows down the relaxation to the S_1 state. This can be partially explained by an increase of the energy gap between S_1 and S_2 due to the presence of methanol with respect to that in vacuum (see Supplemental **Figure S1**), revealing differential relative stabilization of these states by the solvent. The addition of more than 5 methanol molecules to the QM region has negligible effects.

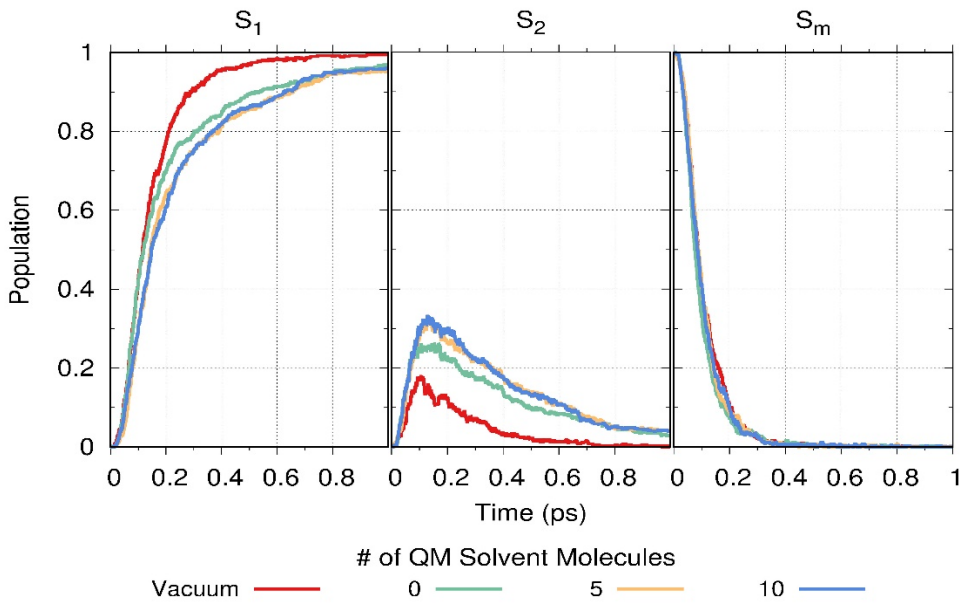

Figure 3. Comparison of the time-evolution of the average populations of different electronic states after the initial photoexcitation to the S_m band for simulations in vacuum and in methanol with varying number of solvent molecules included in the QM region.

The rise of the population on S_1 state was then fitted to a function

$$f(t) = 1 - \left(Ae^{-t/\tau_1} + (1-A)e^{-t/\tau_2}\right) \qquad (5)$$

The results in **Table I**, show that the rise to S_1 slows down in the presence of methanol. As before (**Figure 2**), the addition of more than 5 methanol molecules in the QM region does not substantially change the rise rate.

Table 1. Fitting parameters, according to eq. 5, for the S_1 rise times for PPV3-NO_2 in vacuum and methanol with different number of methanol solvents included in the QM region (0 (vacuum), 5 and 10.

	Vacuum	**MM**	**MM/5**	**MM/10**
A	0	0.193	0.198	0.176
$\boldsymbol{\tau_1}$ (fs^{-1})	-	500.0	495.7	494.4
$\boldsymbol{\tau_2}$ (fs^{-1})	149.2	150.0	191.8	198.7

Bond length alternation

The fast structural response to the electronic relaxation can be inferred by analyzing C-C bond stretching motions commonly characterized by the bond length alternation (BLA) parameter, defined as

$$\frac{d_A+d_B}{2} - d_C \qquad (6)$$

where d_A and d_B are d_1 and d_3 (d_4 and d_6), and d_C is d_2 (d_5) are shown in **Figure 1, top panel**. BLA values reflect the inhomogeneity in the distribution of π-electrons along the bonds in a conjugated molecule. Smaller values of BLA are associated with better π-conjugation between neighboring phenyl rings and, therefore, an improved electronic delocalization.

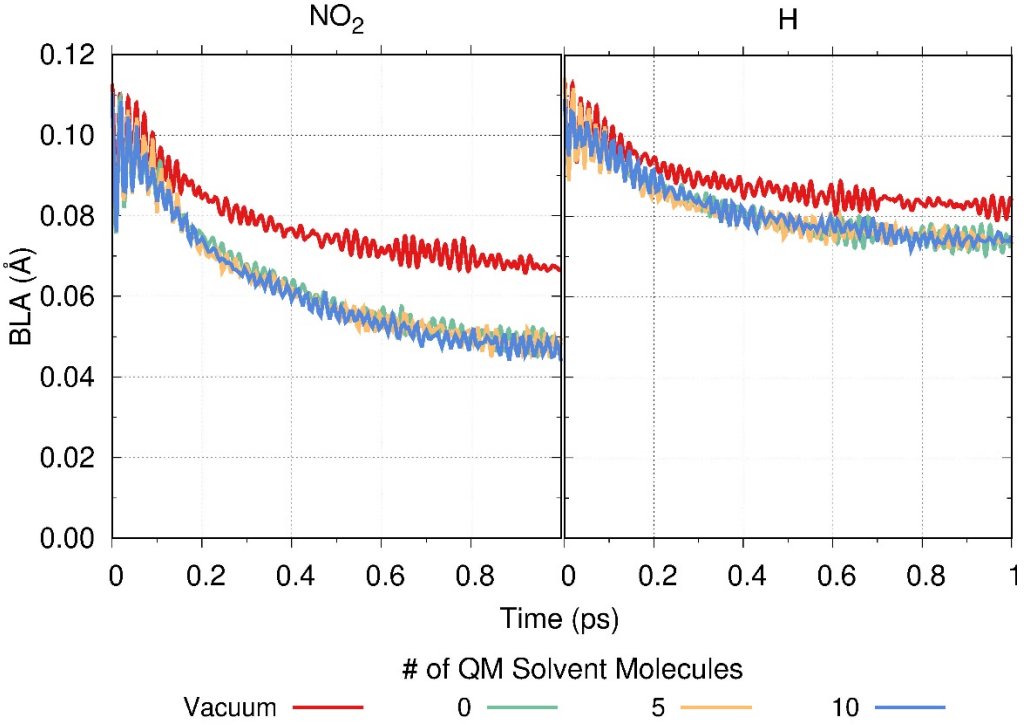

Figure 4. Evolution in time of the BLA of bonds $d_{1\text{-}3}$ and $d_{4\text{-}6}$ during nonadiabatic excited state molecular dynamics simulation with varying number of solvent molecules included in the QM region.

Figure 4 shows that the nuclear reorganization is concomitant to the electronic relaxation, being more pronounced when PPV3-NO2 is embedded in methanol and the further addition of methanol molecules to the QM region does not have a significant impact. The reorganization is significantly larger, i.e. smaller values of BLA, in bonds $d_{1\text{-}3}$ (see **Figure 1**) with respect to $d_{4\text{-}6}$. This indicates a better π-conjugation and, therefore, an additional spatial energy stabilization at the side of the molecule with the $-NO_2$ group with respect to the opposite side. The slightly higher values with respect to simulations performed in implicit solvent[55] indicate that explicit solvent moderately suppresses electronic delocalization due to electrostatic screening coming from the surrounding solvent molecules point charges. Nevertheless, the final values for S_1 state remain higher to the average values of BLA ~0.11Å during ground state molecular dynamics simulations[55].

Bond Orders.

The nuclear reorganization during the non-adiabatic dynamics revealed by the decrease of the values of BLAs should also be reflected in changes of Wiberg bond orders[77,78] that provides a reasonable analogy of the classical Lewis structure and can be calculated from the elements of ground ($\boldsymbol{\rho}_{00}$) and excited ($\boldsymbol{\rho}_{\alpha\alpha}$) state density matrix elements as

$$W_{AB} = \sum_{\mu \in A} \sum_{\nu \in B} \left| (\rho_{\alpha\alpha})_{\mu\nu} \right|^2 \qquad (7)$$

where A and B are indexes of the two bonded atoms, μ and ν are atomic orbitals in those atoms, and $(\rho_{\alpha\alpha})_{\mu\nu}$ are the density matrix elements. The method sums the electron density shared by both atoms. Values ~1 and ~2 are associated with the single and double bonds, respectively. Error! Reference source not found. displays the bond orders of bonds d_1 to d_6 for PPV3-NO_2 in vacuum and embedded in methanol with different number of methanol molecules included in the QM region. During the excited-state dynamics, d_1, d_3, d_4, d_6 bonds slowly increase their values of W_{AB} and gain more double-bond character while d_2 and d_5 bonds reduce their corresponding values and gain more single-bond character. This confirms our observations of a more effective π-conjugation in the excited states with respect to the ground state. The effect is more significant at the substituted side of the molecule with ($d_{1\text{-}3}$) with respect to the side with ($d_{4\text{-}6}$). In fact, the solvent amplifies the changes observed during the photoinduced dynamics in vacuum. This parallels changes in the nuclear reorganization evidenced by the BLA values in **Figure 4**. As stated before, the further addition of methanol molecules to the QM regions does not have a significant effect on these results.

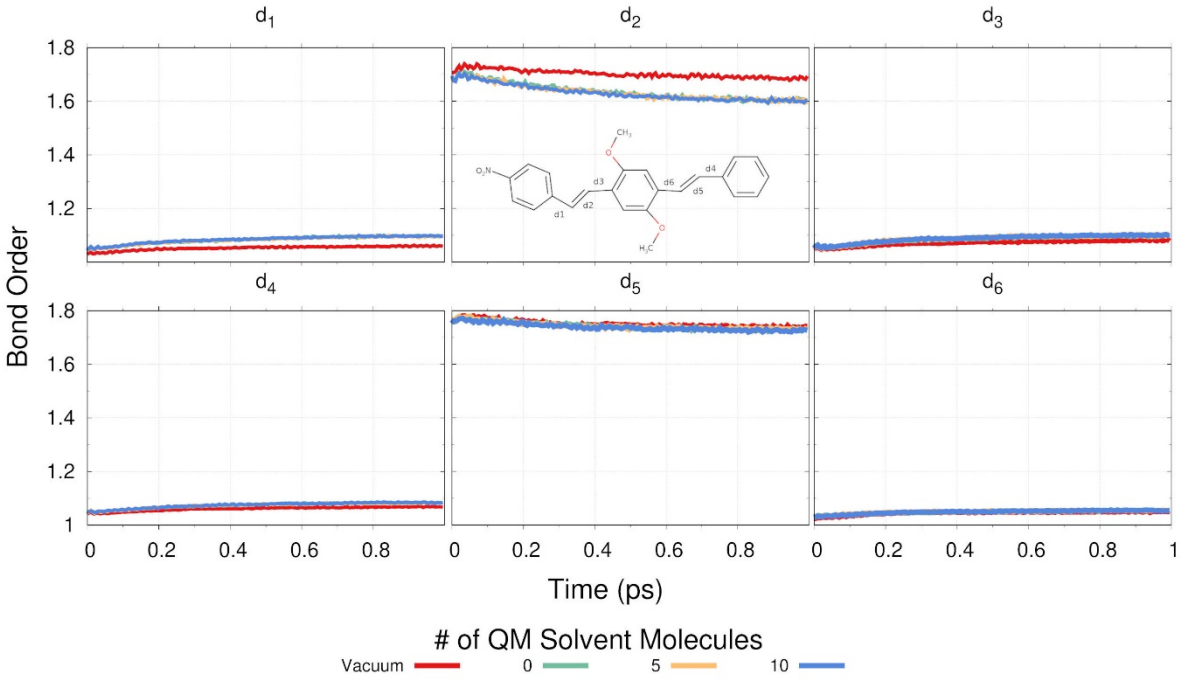

Figure 5. Evolution in time of Wiberg bond orders for bonds d_1 to d_6 during nonadiabatic excited state molecular dynamics simulation in vacuum and in methanol with varying number of solvent molecules included in the QM region.

Excited state planarization

Excited-state dynamics leads to nuclear reorganizations that tend to a more effective π-conjugation, as it has been reflected by changes in BLA and W_{AB}. Concomitant to these changes, multiple experimental and theoretical studies in conjugated chromophores[79, 80, 81, 82,83, 84, 85, 86] reported excited state planarization during dynamics of π– π* electronic excitations. **Figure 6** displays the evolution in time of the average dihedral angles of rotations around d_1/d_3 and d_4/d_6 bonds during the non-adiabatic relaxation of PPV3-NO_2 in vacuum and in methanol with different number of methanol molecules included in the QM region. The ground state structures equilibrated at ambient conditions in methanol have in average ~5º smaller compared to the corresponding geometries obtained in vacuum. After photoexcitation, changes in the dihedral angle indicate an ultrafast planarization occurring both in vacuum and in methanol environment. As it has been shown for changes in BLA and W_{AB}, the solvent effects are larger at the side of the molecule substituted with -NO_2. Additionally, the impact of adding methanol molecules to the QM region is larger in the former with respect to the latter. The final average values of ~12º and ~16º, compared to the equilibrated values obtained in our previous adiabatic simulations on S_1,[55] indicates that after 1ps of simulations after photoexcitation to the S_m band is close to its final equilibrated state at S_1.

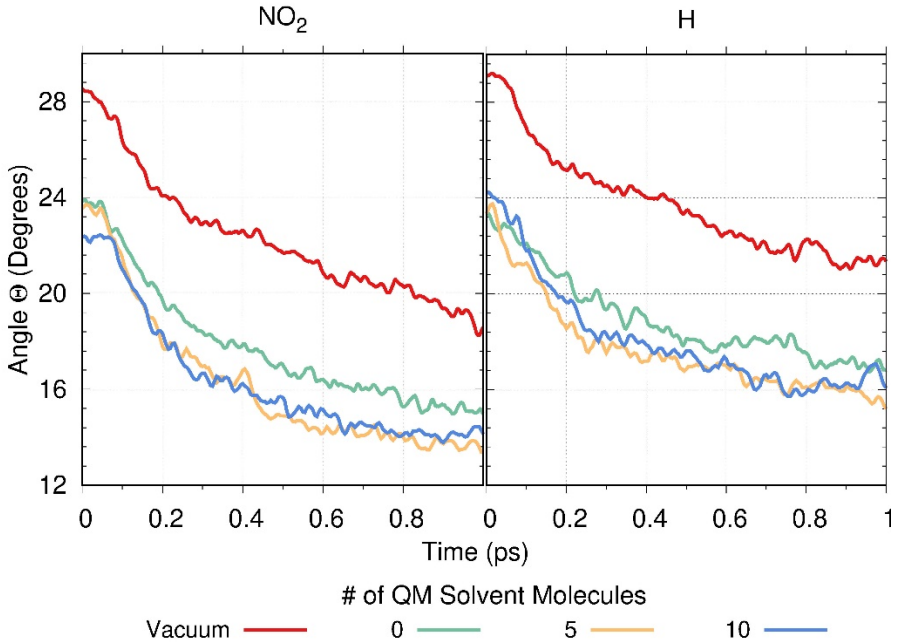

Figure 6. Evolution in time of the dihedral angle around d_1/d_3, i.e. at the side of the molecule with the -NO_2 group, and around d_4/d_6 at the size without it during nonadiabatic excited state molecular dynamics simulation in vacuum and in methanol with varying number of solvent molecules included in the QM region.

I. CONCLUSIONS

We report a NEXMD-SANDER QM/MM implementation as a useful and efficient computational tool to simulate nonadiabatic excited-state molecular dynamics simulations of molecular systems involving manifolds of coupled electronic excited states over picoseconds timescales in the presence of explicit solvent. Our implementation allows the analysis of nuclear reorganizations that take place concomitant to the internal conversion processes. Following our previous implementations of implicit solvent[20] and adiabatic excited-state molecular simulations[55], the acceptor-substituted conjugated oligomer (PPV3-NO_2) has been considered as a test case. Values of bond-length alternation, bond order and dihedral angles changes vary according to the internal conversion process from the S_m band to the lowest S_1 excited state. These changes are more pronounced at the side of the molecule with the polar $-NO_2$ group, similar to what has been observed in adiabatic excited-state dynamics. In this example, including more than 5 methanol molecules as QM does not introduce significant additional solvent effects. The comparison of these simulations with respect to the corresponding modeling that uses implicit solvents or/and simulations performed using adiabatic excited-state molecular dynamics provides insights on the effects of specific solute−solvent interactions and impact of initial excess of energy added by laser excitation on the solute properties. Altogether, our NEXMD-SANDER QM/MM implementation encourages future nonadiabatic excited-state simulation on multichromophoric molecular systems in solution experiencing processes like electron transfer, stabilization of charge separated excited states, and solvent induced reorganization in the molecular optical properties observed in solution-based time-resolved spectroscopic experiments.

Notes

The authors declare no competing financial interest. The Non-adiabatic EXcited state molecular dynamics (NEXMD) Program code, license, and documentation may be accessed at http://github.com/lanl/NEXMD.

Supporting Information

Figure S1 shows average values of the energy gaps between states at the moment of energy transfer (i.e. non-adiabatic 'hops') between them.

Acknowledgements

This work was partially supported in part by CONICET, UNQ, ANPCyT (PICT-2018-2360). The work at Los Alamos National Laboratory (LANL) was performed in part at the Center for Integrated Nanotechnologies (CINT), an Office of Science User Facility of the U.S. Department of Energy. The authors acknowledge University of Florida Research

Computing for providing computational resources and support that have contributed to the research results reported in this publication. URL: http://researchcomputing.ufl.edu

BIBLIOGRAPHY

(1) Lo, S.-C.; Burn, P. L. Development of Dendrimers: Macromolecules for Use in Organic Light-Emitting Diodes and Solar Cells. *Chem. Rev.* **2007**, *107* (4), 1097–1116.

(2) Scholes, G.; Fleming, G.; Olaya-Castro, A.; van Grondelle, R. Lessons from Nature about Solar Light Harvesting. *Nat. Chem.* **2011**, *3* (10), 763–774.

(3) Hedley, G. J.; Ruseckas, A.; Samuel, I. D. W. Light Harvesting for Organic Photovoltaics. *Chem. Rev.* **2017**, *117* (2), 796–837.

(4) Kohler, A. .; Bassler, H. *Electronic Processes in Organic Semiconductors: An Introduction*; John Wiley & Sons: Weinheim, Germany, 2015.

(5) Ingana¨s, O. Organic Photovoltaics over Three Decades. *Adv. Mater.* **2018**, *30*, 1800388.

(6) Lee, H. .; Kim, J. .; Kim, H.-H. .; Kim, C.-S. .; Kim, J. Review on Optical Imaging Techniques for Multispectral Analysis of Nanomaterials. *Nanotheranostics* **2022**, *6* (1), 50–61.

(7) Liyan, C.; Di, W.; Juyoung, Y. Recent Advances in the Development of Chromophore-Based Chemosensors for Nerve Agents and Phosgene. *ACS Sens.* **2018**, *3*, 27–43.

(8) Morzan, U. N.; Alonso De Armiño, D. J.; Foglia, N. O.; Ramírez, F.; González Lebrero, M. C.; Scherlis, D. A.; Estrin, D. A. Spectroscopy in Complex Environments from QM-MM Simulations. *Chem. Rev.* **2018**, *118* (7), 4071–4113. https://doi.org/10.1021/acs.chemrev.8b00026.

(9) Balevičius, V.; Wei, T.; Di Tommaso, D.; Abramavicius, D.; Hauer, J.; Polívka, T.; Duffy, C. D. P. The Full Dynamics of Energy Relaxation in Large Organic Molecules: From Photo-Excitation to Solvent Heating. *Chem. Sci.* **2019**, *10* (18), 4792–4804. https://doi.org/10.1039/c9sc00410f.

(10) Nelson, T. R.; White, A. J.; Bjorgaard, J. A.; Sifain, A. E.; Zhang, Y.; Nebgen, B.; Fernandez-alberti, S.; Mozyrsky, D.; Roitberg, A. E.; Tretiak, S. Non-Adiabatic Excited-State Molecular Dynamics : Theory and Applications for Modeling Photophysics in Extended Molecular Materials. *Chem. Rev.* **2020**, *120* (4), 2215–2287. https://doi.org/10.1021/acs.chemrev.9b00447.

(11) Kumpulainen, T.; Lang, B.; Rosspeintner, A.; Vauthey, E. Ultrafast Elementary

Photochemical Processes of Organic Molecules in Liquid Solution. *Chem. Rev.* **2017**, *117* (16), 10826–10939. https://doi.org/10.1021/acs.chemrev.6b00491.

(12) Park, K. H.; Kim, W.; Yang, J.; Kim, D. Excited-State Structural Relaxation and Exciton Delocalization Dynamics in Linear and Cyclic π-Conjugated Oligothiophenes. *Chem. Soc. Rev.* **2018**, *47* (12), 4279–4294. https://doi.org/10.1039/c7cs00605e.

(13) Jaiswal, V. K.; Kabaciński, P.; Nogueira De Faria, B. E.; Gentile, M.; De Paula, A. M.; Borrego-Varillas, R.; Nenov, A.; Conti, I.; Cerullo, G.; Garavelli, M. Environment-Driven Coherent Population Transfer Governs the Ultrafast Photophysics of Tryptophan. *J. Am. Chem. Soc.* **2022**, *144* (28), 12884–12892. https://doi.org/10.1021/jacs.2c04565.

(14) Grozema, F. C.; Swart, M.; Zijlstra, R. W. J.; Piet, J. J.; Siebbeles, L. D. A.; Van Duijnen, P. T. QM/MM Study of the Role of the Solvent in the Formation of the Charge Separated Excited State in 9,9′-Bianthryl. *J. Am. Chem. Soc.* **2005**, *127* (31), 11019–11028. https://doi.org/10.1021/ja051729g.

(15) Boereboom, J. M.; Fleurat-Lessard, P.; Bulo, R. E. Explicit Solvation Matters: Performance of QM/MM Solvation Models in Nucleophilic Addition. *J. Chem. Theory Comput.* **2018**, *14* (4), 1841–1852. https://doi.org/10.1021/acs.jctc.7b01206.

(16) Virshup, A. M.; Punwong, C.; Pogorelov, T. V; Lindquist, B. A.; Ko, C.; Martinez, T. J. Photodynamics in Complex Environments: Ab Initio Multiple Spawning Quantum Mechanical/Molecular Mechanical Dynamics. *J. Phys. Chem. B* **2009**, *113* (11), 3280–3291.

(17) Toldo, J. M.; Do Casal, M. T.; Ventura, E.; Do Monte, S. A.; Barbatti, M. Surface Hopping Modeling of Charge and Energy Transfer in Complex Environments. *Phys. Chem. Chem. Phys.* **2023**, *25*, 8293–8316. https://doi.org/10.1039/d3cp00247k.

(18) Palombo, R.; Barneschi, L.; Pedraza-González, L.; Padula, D.; Schapiro, I.; Olivucci, M. Retinal Chromophore Charge Delocalization and Confinement Explain the Extreme Photophysics of Neorhodopsin. *Nat. Comm.* **2022**, *13*, 6652. https://doi.org/10.1038/s41467-022-33953-y.

(19) Yang, X.; Manathunga, M.; Gozem, S.; Léonard, J.; Andruniów, T.; Olivucci, M. Quantum–Classical Simulations of Rhodopsin Reveal Excited-State Population Splitting and Its Effects on Quantum Efficiency. *Nat. Chem.* **2022**, *14* (April), 441–449. https://doi.org/10.1038/s41557-022-00892-6.

(20) Sifain, A.; Bjorgaard, J.; Nelson, T.; Nebgen, B.; White, A.; Gifford, B.; Gao, D.; Prezhdo, O.; Fernandez-Alberti, S.; Roitberg, A.; Tretiak, S. Photoexcited Nonadiabatic Dynamics of Solvated Push-Pull π-Conjugated Oligomers with the NEXMD Software. *J. Chem. Theory Comput.* **2018**, *14*, 3955–3966.

(21) Bjorgaard, J. A.; Nelson, T.; Kalinin, K.; Kuzmenko, V.; Velizhanin, K. A.; Tretiak, S. Simulations of Fluorescence Solvatochromism in Substituted PPV Oligomers

from Excited State Molecular Dynamics with Implicit Solvent. *Chem. Phys. Lett.* **2015**, *631–632*, 66–69. https://doi.org/10.1016/j.cplett.2015.04.030.

(22) Mennucci, B.; Tomasi, J. Continuum Solvation Models: A New Approach to the Problem of Solute's Charge Distribution and Cavity Boundaries. *J. Chem. Phys.* **1997**, *106*, 5151−5158.

(23) Cossi, M.; Barone, V.; Cammi, R.; Tomasi, J. Ab Initio Study of Solvated Molecules: A New Implementation of the Polarizable Continuum Model. *Chem. Phys. Lett.* **1996**, *255*, 327−335.

(24) Bjorgaard, J. A.; Kuzmenko, V.; Velizhanin, K. A.; Tretiak, S. Solvent Effects in Time-Dependent Self-Consistent Field Methods. I. Optical Response Calculations. *J. Chem. Phys.* **2015**, *142*, 044103.

(25) Forde, A.; Freixas, V. M.; Fernandez-alberti, S.; Neukirch, A. J.; Tretiak, S. Charge-Transfer Luminescence in a Molecular Donor − Acceptor Complex: Computational Insights. *J. Phys. Chem. Lett.* **2022**, *13*, 8755−8760. https://doi.org/10.1021/acs.jpclett.2c02479.

(26) Giuliani, G.; Melaccio, F.; Gozem, S.; Cappelli, A.; Olivucci, M. QM/MM Investigation of the Spectroscopic Properties of the Fluorophore of Bacterial Luciferase. *J. Chem. Theory Comput.* **2021**, *17*, 605–613. https://doi.org/10.1021/acs.jctc.0c01078.

(27) Blanco-Gonzalez, A.; Manathunga, M.; Yang, Xuchun;Olivucci, M. Comparative Quantum-Classical Dynamics of Natural and Synthetic Molecular Rotors Show How Vibrational Synchronization Modulates the Photoisomerization Quantum Ef Fi Ciency. *Nat. Comm.* **2024**, *15*, 3499. https://doi.org/10.1038/s41467-024-47477-0.

(28) Pedraza-Gonzalez, L.; Barneschi, L.; Marszałek, M.; Padula, D.; Vico, L. De; Olivucci, M. Automated QM / MM Screening of Rhodopsin Variants with Enhanced Fluorescence. *J. Chem. Theory Comput. Comput.* **2023**, *19*, 293–310. https://doi.org/10.1021/acs.jctc.2c00928.

(29) Field, M. J.; Bash, P. A.; Karplus, M. A Combined Quantum Mechanical and Molecular Mechanical Potential for Molecular Dynamics Simulations. *J. Comput. Chem.* **1990**, *11*, 700−733.

(30) Gao, J.; Truhlar, D. G. Quantum Mechanical Methods for Enzyme Kinetics. *Annu. Rev. Phys. Chem.* **2002**, *53*, 467−505.

(31) Liu, M.; Wang, Y.; Chen, Y.; Field, M. J.; Gao, J. QM/MM through the 1990s: The First Twenty Years of Method Development and Applications. *Isr. J. Chem.* **2014**, *54* (8–9), 1250–1263. https://doi.org/10.1002/ijch.201400036.

(32) Avagliano, D.; Conti, I.; Chemistry, I.; Montanari, T. *Hybrid QM / MM Approach for the Calculation of Excited States in Complex Environments*; Elsevier Ltd., 2023. https://doi.org/10.1016/B978-0-12-821978-2.00059-3.

(33) Csizi, K.; Reiher, M. Universal QM / MM Approaches for General Nanoscale Applications. *WIREs Comput. Mol. Sci.* **2023**, *e1656* (November 2022), 1–29. https://doi.org/10.1002/wcms.1656.

(34) Segatta, F.; Cupellini, L.; Garavelli, M.; Mennucci, B. Quantum Chemical Modeling of the Photoinduced Activity of Multichromophoric Biosystems. *Chem. Rev.* **2019**, *119*, 9361–9380. https://doi.org/10.1021/acs.chemrev.9b00135.

(35) Curchod, B. F. E.; Martínez, T. J. Ab Initio Nonadiabatic Quantum Molecular Dynamics. *Chem. Rev.* **2018**, *118* (7), 3305–3336. https://doi.org/10.1021/acs.chemrev.7b00423.

(36) Cerezo, J.; Liu, Y.; Lin, N.; Zhao, X.; Improta, R.; Santoro, F. Mixed Quantum/Classical Method for Nonadiabatic Quantum Dynamics in Explicit Solvent Models: The Ππ∗/Nπ∗ Decay of Thymine in Water as a Test Case. *J. Chem. Theory Comput.* **2018**, *14* (2), 820–832. https://doi.org/10.1021/acs.jctc.7b01015.

(37) Gulak, M. F.; Min, S. K.; Paolino, M.; Kaliakin, D.; Olivucci, M.; Kraka, E.; Min, S. K. Impact of Solvation on the Photoisomerisation Dynamics of a Photon- Only Rotary Molecular Motor. *Commun. Phys.* **2024**, *7*, 219. https://doi.org/10.1038/s42005-024-01716-4.

(38) Avagliano, D.; Bonfanti, M.; Garavelli, M.; González, L. QM/MM Nonadiabatic Dynamics: The SHARC/COBRAMM Approach. *J. Chem. Theory Comput.* **2021**, *17* (8), 4639–4647. https://doi.org/10.1021/acs.jctc.1c00318.

(39) Nogueira, J. J.; Gonz, L. Computational Photophysics in the Presence of an Environment. *Annu. Rev. Phys. Chem.* **2018**, *69*, 473–497.

(40) Bondanza, M.; Demoulin, B.; Lipparini, F.; Barbatti, M.; Mennucci, B. Trajectory Surface Hopping for a Polarizable Embedding QM / MM Formulation. *J. Phys. Chem. A* **2022**, *126*, 6780–6789. https://doi.org/10.1021/acs.jpca.2c04756.

(41) Cofer-shabica, D. V.; Menger, M. F. S. J.; Ou, Q.; Shao, Y.; Subotnik, J. E.; Faraji, S. INAQS , a Generic Interface for Nonadiabatic QM / MM Dynamics : Design , Implementation , and Validation for GROMACS / Q-CHEM Simulations. *J. Chem. Theor. Comput.* **2022**, *18*, 4601–4614. https://doi.org/10.1021/acs.jctc.2c00204.

(42) Liu, X.; Chemistry, C.; Science, M. *Photochemistry of Biological Systems : Excited-State Electronic Structure Calculations and Nonadiabatic Dynamics Simulations with QM / MM Methods*; Elsevier Ltd., 2022. https://doi.org/10.1016/B978-0-12-821978-2.00047-7.

(43) Crespo-Otero, R.; Barbatti, M. Recent Advances and Perspectives on Nonadiabatic Mixed Quantum-Classical Dynamics. *Chem. Rev.* **2018**, *118* (15), 7026–7068. https://doi.org/10.1021/acs.chemrev.7b00577.

(44) Atkins, A. J.; González, L. Trajectory Surface-Hopping Dynamics Including Intersystem Crossing in [Ru(Bpy)3]2+. *J. Phys. Chem. Lett.* **2017**, *8* (16), 3840–3845. https://doi.org/10.1021/acs.jpclett.7b01479.

(45) Ruckenbauer, M.; Barbatti, M.; Müller, T.; Lischka, H. Nonadiabatic Photodynamics of a Retinal Model in Polar and Nonpolar Environment. *J. Phys. Chem. A* **2013**, *117* (13), 2790–2799. https://doi.org/10.1021/jp400401f.

(46) Barbatti, M.; Granucci, G.; Persico, M.; Ruckenbauer, M.; Vazdar, M.; Eckert-Maksić, M.; Lischka, H. The On-the-Fly Surface-Hopping Program System Newton-X: Application to Ab Initio Simulation of the Nonadiabatic Photodynamics of Benchmark Systems. *J. Photochem. Photobiol. A Chem.* **2007**, *190* (2–3), 228–240. https://doi.org/10.1016/j.jphotochem.2006.12.008.

(47) Barbatti, M.; Ruckenbauer, M.; Plasser, F.; Pittner, J.; Granucci, G.; Persico, M.; Lischka, H. Newton-X: A Surface-Hopping Program for Nonadiabatic Molecular Dynamics. *Wiley Interdiscip. Rev. Comput. Mol. Sci.* **2014**, *4* (1), 26–33. https://doi.org/10.1002/wcms.1158.

(48) Richter, M.; Marquetand, P.; González-Vázquez, J.; Sola, I.; González, L. SHARC: Ab Initio Molecular Dynamics with Surface Hopping in the Adiabatic Representation Including Arbitrary Couplings. *J. Chem. Theory Comput.* **2011**, *7* (5), 1253–1258. https://doi.org/10.1021/ct1007394.

(49) Mai, S.; Marquetand, P.; González, L. Nonadiabatic Dynamics: The SHARC Approach. *Wiley Interdiscip. Rev. Comput. Mol. Sci.* **2018**, *8* (6), 1–23. https://doi.org/10.1002/wcms.1370.

(50) Akimov, A. V.; Prezhdo, O. V. The PYXAID Program for Non-Adiabatic Molecular Dynamics in Condensed Matter Systemsmics in Condensed Matter Systems. *J. Chem. Theory Comput.* **2013**, *9* (11), 4959–4972. https://doi.org/10.1021/ct400641n.

(51) Akimov, A. V.; Prezhdo, O. V. Advanced Capabilities of the PYXAID Program: Integration Schemes, Decoherence Effects, Multiexcitonic States, and Field-Matter Interaction. *J. Chem. Theory Comput.* **2014**, *10* (2), 789–804. https://doi.org/10.1021/ct400934c.

(52) Malone, W.; Nebgen, B.; White, A.; Zhang, Y.; Song, H.; Bjorgaard, J. A.; Sifain, A. E.; Rodriguez-Hernandez, B.; Freixas, V. M.; Fernandez-Alberti, S. NEXMD Software Package for Non-Adiabatic Excited State Molecular Dynamics Simulations. *J. Chem. Theory Comput.* **2020**.

(53) Du, L.; Lan, Z. An On-the-Fly Surface-Hopping Program JADE for Nonadiabatic Molecular Dynamics of Polyatomic Systems : Implementation and Applications. *J. Chem. Theory Comput.* **2015**, *11*, 1360–1374. https://doi.org/10.1021/ct501106d.

(54) Malone, W.; Nebgen, B.; White, A.; Zhang, Y.; Song, H.; Bjorgaard, J. A.; Sifain, A. E.; Rodriguez-Hernandez, B.; Freixas, V. M.; Fernandez-Alberti, S.; Roitberg, A. E.; Nelson, T. R.; Tretiak, S. NEXMD Software Package for Nonadiabatic Excited State Molecular Dynamics Simulations. *J. Chem. Theory Comput.* **2020**, *16* (9), 5771–5783. https://doi.org/10.1021/acs.jctc.0c00248.

(55) Tracy, D. A.; Fernandez-alberti, S.; Tretiak, S.; Roitberg, A. E. Adiabatic Excited-

State Molecular Dynamics with an Explicit Solvent: NEXMD-SANDER Implementation. *J. Chem. Theory Comput.* **2022**, *18*, 5213–5220. https://doi.org/10.1021/acs.jctc.2c00561.

(56) Case, D. A. .; Ben-Shalom, I. Y. .; Brozell, S. R. .; Cerutti, D. S. .; Cheatham III, T. E. .; Cruzeiro, V. W. D. .; Darden, T. A. .; Duke, R. E. ; Ghoreishi, D. .; Gilson, M. K. .; Gohlke, H. .; Goetz, A. W. .; Greene, D. .; Harris, R. .; Homeyer, N. .; Izadi, S. .; Kovalenko, A. .; Kurtzman, T. .; Lee, T. S. .; LeGra, S. .; York, D. M. .; Kollman, P. A. Amber18. University of California: San Francisco 2018.

(57) J.-L. Brédas and A. Heeger. Influence of Donor and Acceptor Substituents on the Electronic Characteristics of Poly (Paraphenylene Vinylene) and Poly (Paraphenylene). *Chem. Phys. Lett.* **1994**, *217*, 507–512.

(58) Park, Y. Il; Kuo, C. Y.; Martinez, J. S.; Park, Y. S.; Postupna, O.; Zhugayevych, A.; Kim, S.; Park, J.; Tretiak, S.; Wang, H. L. Tailored Electronic Structure and Optical Properties of Conjugated Systems through Aggregates and Dipole-Dipole Interactions. *ACS Appl. Mater. Interfaces* **2013**, *5* (11), 4685–4695. https://doi.org/10.1021/am400766w.

(59) Rauscher, U.; Bässler, H.; Bradley, D. D. C.; Hennecke, M. Exciton versus Band Description of the Absorption and Luminescence Spectra in Poly(p-Phenylenevinylene). *Phys. Rev. B* **1990**, *42* (16), 9830–9836. https://doi.org/10.1103/PhysRevB.42.9830.

(60) Burroughes, J. H.; Bradley, D. D. C.; Brown, A. R.; Marks, R. N.; Mackay, K.; Friend, R. H.; Burns, P. L.; Holmes, A. B. Light-Emitting Diodes Based on Conjugated Polymers. *Nature* **1990**, *347* (6293), 539–541. https://doi.org/10.1038/347539a0.

(61) Vestweber, B. H.; Greiner, A.; Lemmer, U. Progress Towards Processible Materials for Light-Emitting Devices Using Poly(p-Phenylphenylenevilnylene). *Adv. Mat.* **1992**, *4* (10), 661–662.

(62) Cornil, J.; Beljonne, D.; Shuai, Z.; Hagler, T. W.; Campbell, I.; Bradley, D. D. C.; Brédas, J. L.; Spangler, C. W.; Mullen, K. Vibronic Structure In The Optical-Absorption Spectra Of Phenylene Vinylene Oligomers : A Joint Experimental And Theoretical-Study. *Chem. Phys. Lett.* **1995**, *247* (4–6), 425–432.

(63) Freixas, V. M. .; Malone, W. .; Li, X. .; Song, H. .; Negrin-Yuvero, H. .; Pérez-Castillo, R. .; White, A. .; Gibson, T. R. .; Makhov, D. V. .; Shalashilin, D. V.; Zhang, Y. .; Fedik, N. .; Kulichenko, M. .; Messerly, R. .; Mohanam, L. .; Sharifzadeh, S.; Bastida, A. .; Mukamel, S. .; Sebastian Fernandez-Alberti, S. .; AndTretiak, S. NEXMD v2.0 Software Package for Nonadiabatic Excited State Molecular Dynamics Simulations. *J. Chem. Theor. Comput.* **2023**, *19*, 5356–5368.

(64) Tully, J. C. Molecular Dynamics with Electronic Transitions. *J. Chem Phys.* **1990**, *93*, 1061–1071.

(65) Hammes-schiffer, S.; Tully, J. C. Proton Transfer in Solution : Molecular Dynamics with Quantum Transitions. *J. Chem Phys.* **1994**, *101* (6), 4657–4667.

(66) Tretiak, S.; Isborn, C. M.; Niklasson, A. M. N.; Challacombe, M. Representation Independent Algorithms for Molecular Response Calculations in Time-Dependent Self-Consistent Field Theories. *J. Chem. Phys.* **2009**, *130* (5), 054111. https://doi.org/10.1063/1.3068658.

(67) Nelson, T.; Fernandez-Alberti, S.; Roitberg, A. E.; Tretiak, S. Nonadiabatic Excited State Molecular Dynamics: Modeling Photophysics in Organic Conjugated Materials. *Acc. Chem. Res.* **2014**, *47*, 1155–1164.

(68) Walker, R. C.; Crowley, I. F.; Case, D. A. The Implementation of a Fast and Accurate QM/MM Potential Method in Amber. *J. Comput. Chem.* **2008**, *29* (7), 1019–1031. https://doi.org/10.1002/jcc.20857.

(69) Darden, T.; York, D.; Pedersen, L. Particle Mesh Ewald: An N·log(N) Method for Ewald Sums in Large Systems. *J. Chem. Phys.* **1993**, *98* (12), 10089–10092. https://doi.org/10.1063/1.464397.

(70) Essmann, U.; Perera, L.; Berkowitz, M. L.; Darden, T.; Lee, H.; Pedersen, L. G. A Smooth Particle Mesh Ewald Method. *J. Chem. Phys.* **1995**, *103* (19), 8577–8593. https://doi.org/10.1063/1.470117.

(71) Dewar, M. J. S.; Zoebisch, E. G.; Healy, E. F.; Stewart, J. J. P. The Development and Use of Quantum-Mechanical Molecular-Models.76.AM1 - A New General Purpose Quantum-Mechanical Molecular-Model. *J. Am. Chem. Soc.* **1985**, *107*, 3902–3909.

(72) Nelson, T.; Fernandez-alberti, S.; Roitberg, A. E.; Tretiak, S. Conformational Disorder in Energy Transfer : Beyond F ¨ Orster Theory. 1–22.

(73) Nelson, T.; Fernandez-Aberti, S.; Chernyak, V.; Roitberg, A. E.; Tretiak, S. Nonadiabatic Excited-State Molecular Dynamics Modeling of Photoinduced Dynamics in Conjugated Molecules. *J. Phys. Chem. B* **2011**, *115* (18), 5402–5414.

(74) Nelson, T.; Fernandez-Alberti, S.; Chernyak, V.; Roitberg, A. E.; Tretiak, S. Nonadiabatic Excited-State Molecular Dynamics: Numerical Tests of Convergence and Parameters. *J. Chem. Phys.* **2012**, *136* (5), 054108. https://doi.org/10.1063/1.3680565.

(75) Nelson, T.; Fernandez-Alberti, S.; Roitberg, A. E.; Tretiak, S. Nonadiabatic Excited-State Molecular Dynamics: Treatment of Electronic Decoherence. *J. Chem. Phys.* **2013**, *138* (22). https://doi.org/10.1063/1.4809568.

(76) Fernandez-Alberti, S.; Roitberg, A. E.; Nelson, T.; Tretiak, S. Identification of Unavoided Crossings in Nonadiabatic Photoexcited Dynamics Involving Multiple Electronic States in Polyatomic Conjugated Molecules. *J. Chem. Phys.* **2012**, *137* (1), 014512. https://doi.org/10.1063/1.4732536.

(77) Bagchi, B.; Oxtoby, D. W.; Fleming, G. R. Theory of the Time Development of the Stokes Shift in Polar Media. *Chem. Phys.* **1984**, *86* (3), 257–267. https://doi.org/10.1016/0301-0104(84)80014-2.

(78) Mayer, I. Bond Order and Valence Indices: A Personal Account. *J. Comput. Chem.* **2007**, *28* (1), 204–221. https://doi.org/10.1002/jcc.20494.

(79) Oldani, N.; Doorn, S. K.; Tretiak, S.; Fernandez-Alberti, S. Photoinduced Dynamics in Cycloparaphenylenes: Planarization, Electron-Phonon Coupling, Localization and Intra-Ring Migration of the Electronic Excitation. *Phys. Chem. Chem. Phys.* **2017**, *19* (45), 30914–30924.

(80) Rodríguez-Hernández, B.; Ondarse-Álvarez, D.; Oldani, N.; Martínez-Mesa, A.; Uranga-Piña, L.; Tretiak, S.; Fernández-Alberti, S. Modification of Optical Properties and Excited-State Dynamics by Linearizing Cyclic Paraphenylene Chromophores. *J. Phys. Chem. C* **2018**, *122* (29), 16639–16648. https://doi.org/10.1021/acs.jpcc.8b05582.

(81) Clark, J.; Nelson, T.; Tretiak, S.; Cirmi, G.; Lanzani, G. Femtosecond Torsional Relaxation. *Nat. Phys.* **2012**, *8*, 225–231.

(82) Ondarse-Alvarez, D.; Oldani, N.; Tretiak, S.; Fernandez-Alberti, S. Computational Study of Photoexcited Dynamics in Bichromophoric Cross-Shaped Oligofluorene. *J. Phys. Chem. A* **2014**, *118*, 10742–10753.

(83) Tretiak, S.; Saxena, A.; Martin, R.; Bishop, A. Conformational Dynamics of Photoexcited Conjugated Molecules. *Phys. Rev. Lett.* **2002**, *89*, 97402–97406.

(84) Karabunarliev, S.; Baumgarten, M.; Bittner, E.; Mullen, K. Rigorous Franck Condon Absorption and Emission Spectra of Conjugated Oligomers from Quantum Chemistry. *J. Chem. Phys.* **2000**, *113*, 11372–11381.

(85) Franco, I.; Tretiak, S. Electron-Vibrational Dynamics of Photoexcited Polyfluorenes. *J. Am. Chem. Soc.* **2004**, *126* (38), 12130–12140.

(86) Zimmerman, H. E.; Alabugin, I. V. Excited State Energy Distribution and Redistribution and Chemical Reactivity; Mechanistic and Exploratory Organic Photochemistry. *J. Am. Chem. Soc.* **2000**, *122* (5), 952–953. https://doi.org/10.1021/ja9933801.

Supplementary Materials

Supplementary Materials

Nonadiabatic Excited State Molecular Dynamics with explicit solvent: NEXMD-SANDER implementation

Dustin A. Tracy[1], Sebastian Fernandez Alberti[2], Johan Fabian Galindo[3], Sergei Tretiak[4] and Adrian E. Roitberg[1,5*]

[1]Department of Chemistry, University of Florida, Gainesville, Florida 32611, United States
[2]Universidad Nacional de Quilmes/CONICET, Roque Saenz Peña 352, B1876BXD Bernal, Argentina
[3]Departamento de Química, Universidad Nacional de Colombia, Sede Bogotá, 111321 Bogotá, Colombia.
[4]Theoretical Division, Center for Nonlinear Studies (CNLS) and Center for integrated Nanotechnologies (CINT), Los Alamos National Laboratory, Los Alamos, New Mexico 87545, United States
[5]CONICET─Universidad de Buenos Aires, Instituto de Química-Física de los Materiales, Medio Ambiente y Energía (INQUIMAE), Ciudad Universitaria, Pabellón 2, Buenos Aires C1428EHA, Argentina

*corresponding author: roitberg@ufl.edu

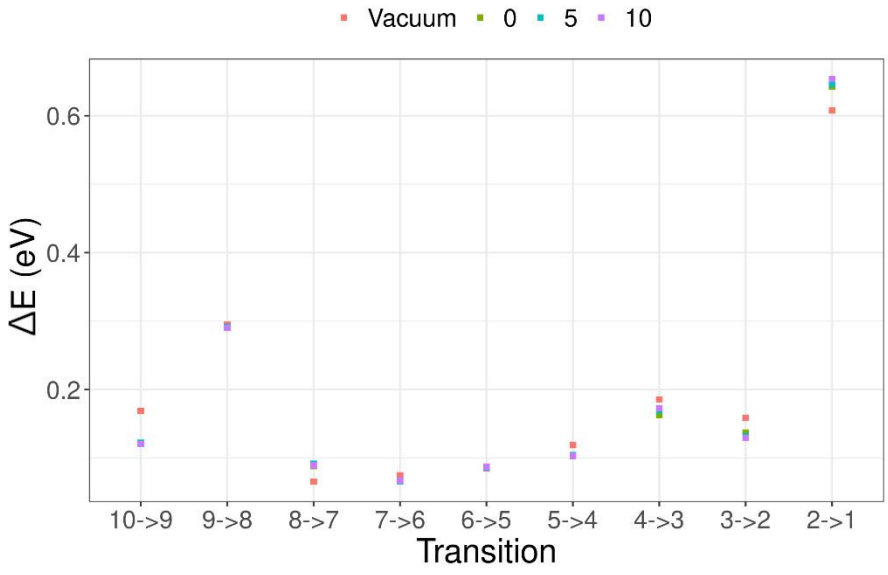

Figure S1. Energy gaps (ΔE) between states at the moment of $S_i \rightarrow S_{i-1}$ hops.